Synthesis, X-ray and optical characterizations of two new oxysulfides: LaInS$_2$O and La$_5$In$_3$S$_9$O$_3$ ☆

H. Kabbour, L. Cario,* Y. Moëlo, and A. Meerschaut

Laboratoire de Chimie des Solides, Université de Nantes, Institut des Matériaux Jean Rouxel, UMR 6502 CNRS, 2, rue de la Houssinière, BP 32229, 44322 Nantes Cedex 03, France

Abstract

Two new compounds, LaInS$_2$O and La$_5$In$_3$S$_9$O$_3$ were synthesized in the La–In–S–O quaternary system. Both compounds crystallize in the orthorhombic system with lattice constants $a = 20.5421(6)$ Å, $b = 14.8490(4)$ Å, $c = 3.9829(1)$ Å for LaInS$_2$O, and $a = 4.1018(1)$ Å, $b = 26.833(1)$ Å, $c = 16.023(1)$ Å for La$_5$In$_3$S$_9$O$_3$. The structure of La$_5$In$_3$S$_9$O$_3$ was solved from single-crystal X-ray data, in the space group *Pbcm*, with $Z = 4$; it is built from three-atom-thick $(100)_{NaCl}$ layers interleaved with fluorite-type ribbons, and is closely related to the structures of the known lanthanum and indium compounds La$_{10}$In$_6$S$_{17}$O$_6$ and La$_4$In$_5$S$_{13}$. Both compounds LaInS$_2$O and La$_5$In$_3$S$_9$O$_3$ exhibit a yellow color; measurement of their optical gaps gave 2.73 and 2.60 eV, respectively.
© 2003 Elsevier Inc. All rights reserved.

Keywords: Oxysulfide; Indium; Lanthanum; Crystal structure; Optical properties

1. Introduction

For a few years the increased importance of transparent conducting compounds for application technologies such as low emissivity windows or thin film photovoltaics led to a renewed interest for this kind of materials [1]. A considerable effort was done to improve existing materials as well as for the search of new materials. Owing to the limitations of existing materials the need for new p-type transparent conducting compounds is especially high. In association with n-type materials, the discovery of efficient p-type materials would open the way to transparent electronics.

Recently, a few new p-type transparent conducting materials have been reported such as SrCuO$_2$ [1] and LaCuSO [2]. LaCuSO presents a composite type structure that results from an alternated stacking of fluorite type layers [La$_2$O$_2$] with anti-fluorite type layers [Cu$_2$S$_2$] [3]. For this compound, band structure calculations show that the valence band is made of Cu and S states while the bottom of the conduction band is made of La states [4]. The p-type conductivity is achieved by replacing part of La by Sr. According to the composite character of the structure, this doping does not alter the conducting [Cu$_2$S$_2$] layer, which could favor a high electrical conductivity.

We have started the search for new p-type transparent conducting compounds with a composite type structure. As In^{3+} is a d^{10} cation with the d energy levels not too far from those of Cu, we have focused our attention on the La–In–S–O system. This paper reports on the chemical, X-ray diffraction and optical characterizations of two new compounds LaInS$_2$O and La$_5$In$_3$S$_9$O$_3$ that we found during our exploration. The crystal structure of La$_5$In$_3$S$_9$O$_3$ has been solved and will be discussed in relation with the homeotypic structure of La$_{10}$In$_6$S$_{17}$O$_6$ [5].

2. Experimental

2.1. Synthesis and chemical analysis

LaInS$_2$O and La$_5$In$_3$S$_9$O$_3$ were obtained during an attempt to synthesize an hypothetical composite compound La$_2$In$_2$S$_4$O$_2$ built from the stacking of both [La$_2$O$_2$] and [InS$_2$] slabs. Powders of La$_2$S$_3$ (preliminary

obtained by sulfurization of La_2O_3 under a gas flow of H_2S at 1200°C), La_2O_3, and In_2S_3 were weighed in a 1:2:3 ratio, respectively. The mixture was loaded into a silica tube sealed under vacuum ($p = 2 \times 10^{-2}$ atm) and heated at a rate of 100°C h^{-1} up to 800°C for 12 h. This reaction yielded a pure yellow powder. The powder was ground and subsequently divided in two equal amounts. Each of them was sealed in an evacuated silica tube and reheated at 850°C or 950°C with a small amount of iodine (< 5 mg cm^{-3}) to favor crystallization. In both cases, a mixture of a yellow powder, black octahedral crystals, and yellow needle-like crystals was obtained.

Chemical analysis by means of energy dispersive X-ray spectrometry (EDXS) revealed that the black octahedral crystals have the composition In_2S_3. For the two yellow phases the chemical analysis confirmed the presence of oxygen and we found the following atomic percentages for the other elements (at%):

- yellow powder La 24.7%, In 23.1%, S 52.2%, in good agreement with the initial composition $LaInS_2O$;
- yellow needle-like crystals La 30.3%, In 14.9%, S 54.8%, in good agreement with the formulation $La_5In_3S_9O_3$ deduced from the single-crystal structure determination (at%: La 29.4, In 17.7, S 52.9).

2.2. Optical measurements

Optical measurements were performed with a Leitz spectrophotometer (MPV-SP), coupled with a metallographic microscope, working in the visible and close IR range (400–800 nm). For $La_5In_3S_9O_3$, two spectra in polarized transmitted light were recorded on a single crystal, with polarization directions perpendicular and parallel to the elongation of the crystal (*a*-axis). On the other hand, the diffuse reflectance spectra of $LaInS_2O$ and In_2S_3 were recorded from powders.

2.3. X-ray powder diffraction

The X-ray powder diffraction pattern of $LaInS_2O$ was recorded on a Bragg–Brentano Siemens D5000 diffractometer. Prior to measurement the yellow powder was ground, passed through a 20 μm mesh, and placed on a flat sample holder.

2.4. Data collection and structure refinement

A single crystal of $La_5In_3S_9O_3$ with a parallelepipedic shape (dimensions $0.005 \times 0.04 \times 0.1$ mm^3) was mounted on a Nonius Kappa CCD diffractometer, using Mo$K\alpha$ radiation ($\lambda = 0.71073$ Å). The crystal-to-detector distance was 40.0 mm. 559 frames were collected with a rotation angle per frame of 0.8° and an exposure time of 92 s. The diffraction pattern was consistent with the

orthorhombic system. We could refine the unit-cell parameter values: $a = 4.1018(1)$ Å, $b = 26.833(1)$ Å, and $c = 16.023(1)$ Å, from 27,948 reflections with $2.91° < \theta < 34.97°$.

Intensities were corrected for absorption ($\mu = 16.73$ mm^{-1}) using the face indexed option. The structure was solved with the use of the direct methods (SHELXS), and refinements with subsequent difference Fourier were done with SHELXL (SHELXTL software package [6]). The structure solution was easily obtained. We had to split an In position into two sites In(2) and In(3) that are too close to be occupied simultaneously. We have then constrained the sum of the occupancies of In(2) and In(3) to be equal to 1, and their thermal parameters to be identical. In the final stage of refinement, i.e., with all atoms (except oxygen atoms) refined anisotropically, the reliability factors converged to $R_1 = 0.0447$ and w$R_2 = 0.0811$ for 1627 observed reflections ($I > 2\sigma(I)$, restricted to $2\theta_{max} = 60°$ ($\sin\theta/\lambda \approx 0.7$)), and 96 parameters. The highest and deepest peaks (4.71 e Å^{-3}; -2.83 e Å^{-3}) on the final Fourier difference map were closed to S(2) (1.43 Å) and La(3) (1.39 Å), respectively. For comparison, the height of the highest residual peak corresponds to about 1/6 of that of an O atom. Details on data collection and structure refinements are given in Table 1. Atomic coordinates and equivalent isotropic displacement parameters are listed in Table 2; coefficients of the anisotropic displacement parameters are listed in

Table 1
Crystal data and structure refinement for $La_5In_3S_9O_3$

Empirical formula	$La_5In_3S_9O_3$
Formula weight (g mol^{-1})	1375.5
Temperature	293(2) K
Wavelength	0.71073 Å
Crystal system	Orthorhombic
Space group	*Pbcm*
Unit-cell dimensions	$a = 4.1018(1)$ Å
	$b = 26.8325(5)$ Å
	$c = 16.0232(3)$ Å
Volume	1763.54(6) Å^3
Z	4
Density (calculated)	5.191 mg/m^3
Absorption coefficient	16.734 mm^{-1}
F(000)	2405
Crystal size	$0.005 \times 0.04 \times 0.1$ mm^3
θ range for data collection	2.54–30.00°
Index ranges	$-5 \leqslant h \leqslant 5$, $-37 \leqslant k \leqslant 37$, $-22 \leqslant l \leqslant 22$
Reflections collected	17520
Independent reflections	2660 [$R_{int} = 0.0903$]
Completeness to $\theta = 30.00°$	99.8%
Refinement method	Full-matrix least-squares on F^2
Data/restraints/parameters	2660/0/96
Goodness-of-fit on F^2	1.145
R indices [1627 $I > 2\sigma(I)$]	$R_1 = 0.0447$, w$R_2 = 0.0811$
R indices (all data)	$R_1 = 0.0951$, w$R_2 = 0.0916$
Extinction coefficient	0.00004(1)
Largest diff. peak and hole	4.72 and -2.83 e Å^{-3}

Table 2
Atomic coordinates and equivalent isotropic displacement parameters ($\text{Å}^2 \times 10^3$) for $La_5In_3O_3S_9$

Atom	Site	S.o.f	x	y	z	U_{eq}
La(1)	8e	1	0.2505(2)	0.5210(1)	0.6198(1)	5(1)
La(2)	4d	1	−0.2498(4)	0.6134(1)	3/4	5(1)
La(3)	8e	1	−0.2530(3)	0.6256(1)	0.4990(1)	6(1)
In(1)	4d	1	−0.2600(5)	0.3820(1)	3/4	11(1)
In(2)	8e	0.852(2)	−0.4284(3)	0.2449(1)	0.6288(1)	11(1)
In(3)	8e	0.148(2)	−0.070(2)	0.2446(2)	0.6287(5)	11(−)
S(1)	8e	1	−0.2403(13)	0.3316(1)	0.6226(2)	10(1)
S(2)	4d	1	0.242(2)	0.4348(1)	3/4	11(1)
S(3)	8e	1	0.2475(13)	0.5534(1)	0.4465(2)	7(1)
S(4)	4c	1	−0.778 (2)	1/4	1/2	12(1)
S(5)	8e	1	−0.7549(13)	0.6582(1)	0.6202(2)	8(1)
S(6)	4d	1	0.214(2)	0.2342(2)	3/4	18(1)
O(1)	4d	1	0.252(5)	0.5606(4)	3/4	7(2)
O(2)	8e	1	−0.248(3)	0.5673(3)	0.6155(5)	7(1)

U_{eq} is defined as one-third of the trace of the orthogonalized U^{ij} tensor.

Table 3
Anisotropic displacement parameters ($\text{Å}^2 \times 10^3$) for $La_5In_3S_9O_3$

	U^{11}	U^{22}	U^{33}	U^{23}	U^{13}	U^{12}
La(1)	4(1)	6(1)	6(1)	−1(1)	0(1)	0(1)
La(2)	4(1)	6(1)	5(1)	0	0	0(1)
La(3)	4(1)	8(1)	7(1)	1(1)	−1(1)	0(1)
In(1)	9(1)	11(1)	12(1)	0	0	−1(1)
In(2)	16(1)	7(1)	10(1)	1(1)	1(1)	0(1)
In(3)	16(1)	7(1)	10(1)	1(1)	1(1)	0(1)
S(1)	12(1)	6(1)	11(1)	0(1)	5(3)	0(2)
S(2)	11(2)	10(2)	12(2)	0	0	0(3)
S(3)	7(1)	7(1)	8(1)	−1(1)	1(2)	−1(2)
S(4)	8(3)	17(2)	12(2)	−2(2)	0	0
S(5)	8(1)	8(1)	8(1)	0(1)	1(3)	−3(2)
S(6)	25(4)	18(2)	9(2)	0	0	2(3)

The anisotropic displacement factor exponent takes the form: $-2\pi^2[h^2a^{*2}U^{11} + \cdots + 2hka^*b^*U^{12}]$.

Table 3. Selected interatomic distances are given in Table 4.

Nota: Considering the tendency for the X-coordinates to be near 1/4 or 3/4, a refinement of the structure in the space group *Cmcm* was performed; it yielded a satisfying reliability factor but too many observed weak reflections violating the C centering mode ($h + k = 2n$) had to be rejected.

2.5. Results and discussion

In the Ln–Ga–S–O system, numerous compounds were reported such as $LaGaS_2O$ [7], La_3GaS_5O [8], $(LaO)_4Ga_{1.33}S_4$ and $(LnO)_4Ga_2S_5$ [9]; the two latter have layered structures formed by alternation of a $[Ln_2O_2]$ slab and a $[Ga_xS_y]$ slab. On the contrary, before our investigation, the only known compound in the quaternary system La–In–S–O was $La_{10}In_6S_{17}O_6$. This compound was synthesized from a mixture of La_2O_2S and In_2S_3 (1:1 ratio) at 1500 K by Gastaldi et al. [5]. At

lower temperature (<1223 K) our investigation of the La–In–S–O quaternary system did not yield $La_{10}In_6S_{17}O_6$ but the two title compounds, namely $LaInS_2O$ and $La_5In_3S_9O_3$.

Fig. 1 gives the X-ray powder pattern of $LaInS_2O$. We could index the pattern in the orthorhombic crystal system (see Table 5), and we have refined the cell parameters as $a = 20.5421(6)$ Å, $b = 14.8490(4)$ Å, $c = 3.9829(1)$ Å using the profile matching mode as implemented in the FullProf software [10]. This compound seems not to be isotypic with $LaGaS_2O$, and we were unable to solve the structure neither using direct methods nor by using a trial and error method.

On the other hand, we were able to solve the structure of $La_5In_3S_9O_3$ which was obtained as single crystals. Fig. 2 shows the structure of this compound projected onto the (**b**, **c**) plane. We observe a segregation of the sulfur and oxygen atoms. Only sulfur atoms coordinate indium atoms, while both oxygen and sulfur atoms coordinate lanthanum atoms. In(1) and In(2)/In(3) atoms are found in tetrahedral coordination of sulfur atoms with In–S distances ranging from 2.28 to 2.52 Å (see Table 4). The sum of the occupancies for In(2) and In(3) was constrained to be equal to 1, which forbids, statistically, the simultaneous occupation of both sites, and then the too short In(2)–In(3) contacts of 1.472 and 2.631 Å, along the **a** direction; the filling is 85.2% and 14.8% for In(2) and In(3), respectively.

As In(2) and In(3) atoms could be ordered along the **a**-direction, we have checked for the existence of a superstructure along this direction. Precession photographs obtained on the Kappa CCD diffractometer did not reveal any superstructure along **a*** that would indicate a long range order for the distribution of the filled In(2) and In(3) sites.

La(1) is seven-fold coordinated (1 O(1), 2 O(2), 3 S(3), and 1 S(2)), with four atoms in an equatorial plane (2 O(2), 2 S(3)) and three other atoms (O(1), S(2), S(3))

Table 4
Bond lengths (Å) and bond valence sums for $La_5In_3S_9O_3$

Atom1	Atom2	Sym.	Distance	Bond val.
La(1)	O(1)		2.340(5)	0.64
La(1)	O(2)		2.392(11)	0.55
La(1)	O(2)	#1	2.405(11)	0.53
La(1)	S(3)		2.910(3)	0.48
La(1)	S(3)	#2	3.048(4)	0.33
La(1)	S(3)	#3	3.059(4)	0.32
La(1)	S(2)		3.115(3)	0.28
La(1)	La(2)	#1	3.8336(14)	—
La(1)	La(3)	#1	3.9710(11)	—
				$\Sigma = 3.13$
La(2)	O(2)		2.485(8)	0.43
La(2)	O(2)	#4	2.485(8)	0.43
La(2)	O(1)	#5	2.489(18)	0.42
La(2)	O(1)		2.497(17)	0.42
La(2)	S(5)	#1	3.145(4)	0.26
La(2)	S(5)	#6	3.145(4)	0.25
La(2)	S(5)	#4	3.172(4)	0.24
La(2)	S(5)		3.172(4)	0.24
La(2)	S(6)	#7	3.244(5)	0.20
				$\Sigma = 2.89$
La(3)	O(2)		2.436(7)	0.49
La(3)	S(3)	#5	2.943(4)	0.44
La(3)	S(3)		2.946(4)	0.44
La(3)	S(5)	#1	2.951(4)	0.43
La(3)	S(5)		2.962(4)	0.42
La(3)	S(1)	#2	3.034(4)	0.34
La(3)	S(1)	#9	3.071(4)	0.31
La(3)	S(4)	#9	3.3399(7)	0.15
La(3)	La(1)	#5	3.9712(11)	—
				$\Sigma = 3.02$
In(1)	S(1)		2.451(3)	0.78
In(1)	S(1)	#4	2.451(3)	0.78
In(1)	S(2)	#5	2.486(7)	0.71
In(1)	S(2)		2.499(7)	0.69
				$\Sigma = 2.96$
In(2)	In(3)		1.472(7)	—
In(2)	S(5)	#10	2.448(3)	0.79
In(2)	S(6)	#5	2.451(5)	0.78
In(2)	S(1)		2.454(3)	0.78
In(2)	S(4)		2.518(4)	0.65
In(2)	In(3)	#5	2.630(7)	—
				$\Sigma = 3.00$
In(3)	S(6)		2.283(9)	1.23
In(3)	S(4)	#1	2.388(8)	0.93
In(3)	S(5)	#10	2.431(7)	0.83
In(3)	S(1)		2.440(7)	0.81
In(3)	In(2)	#1	2.630(7)	—
				$\Sigma = 3.80$

Symmetry transformations used to generate equivalent atoms: #1 $x+1$, y,z; #2 $-x,-y+1,-z+1$; #3 $-x+1,-y+1,-z+1$; #4 $x,y,-z+3/2$; #5 $x-1,y,z$; #6 $x+1,y,-z+3/2$; #7 $-x,y+1/2,-z+3/2$; #9 $-x-1,-y+1,-z+1$; #10 $-x-1$, $y-1/2,z$.

in a perpendicular plane. This arrangement is usually described as a seven-octahedron with one apex split into two positions. La(2) is nine-fold coordinated (2 O(1), 2 O(2), 4 S(5), and 1 S(6)), which corresponds to a tricapped (O(2), O(2), S(6)) trigonal prism. Finally,

La(3) is eight-fold coordinated (O(2), 2 S(1), 2 S(3), 2 S(5), and 1 S(4)), which is identified as the classical bicapped (O(2), S(4)) trigonal prism. The La–S and La–O distances range from 2.91 to 3.34 and 2.34 to 2.50 Å, respectively, as usually observed in lanthanum oxysulfides.

As shown in Fig. 3a, the crystal structure of $La_5In_3S_9O_3$ can be described as the combination of two types of building blocks. The first type is a distorted derivative of a three-atom-thick $(100)_{NaCl}$ layer, with composition $La_{1.5}In_{1.5}S_3$. The second building block is a two-atom-thick, two-tetrahedra-large ribbon of the fluorite type, with composition $[La_5O_3]$. The fluorite building blocks share La atoms on each side of the 2D infinite NaCl-type building block to form a zigzag pattern. Taking into account common La atoms, the connection of both building blocks corresponds to 2D infinite $La_5In_3S_6O_3$ layers. These layers alternate regularly along the **b**-direction with a corrugated S mono-atomic layer.

This description of the structure with building blocks is very useful to highlight the similarity with the high-temperature homeotypic structure of $La_{10}In_6S_{17}O_6$. Indeed, this compound can be described in the same way, but here the layered NaCl-type building block acts as a mirror plane regarding to the fluorite building block, changing the space group from Pbcm to Immm (see Fig. 3b). Another difference between the title compound and $La_{10}In_6S_{17}O_6$ is the lack of one S atom in the inner atomic slab of the layered NaCl-type building block of $La_{10}In_6S_{17}O_6$. This leads to an indium pairing with an In–In distance of 2.86 Å close to two times the covalent radius of indium (3.00 Å). For $La_5In_3S_9O_3$, the corresponding In atoms (i.e. the two adjacent In(2)/In(3) couples along the **c**-direction) are separated by one S(6) atom (see Fig. 2), and the resulting In–In distance is greater than 3.8 Å. Finally both compounds $La_5In_3S_9O_3$ and $La_{10}In_6S_{17}O_6$ are derivatives of $La_4In_5S_{13}$ [11]. This last structure can be described as composed of a layer derived from a three-atom-thick $(100)_{NaCl}$ slab, with composition $La_4In_5S_9$ $[= (La_2InS_3)(In_3S_3)(La_2InS_3)]$, alternating with a sulfur mono-atomic plane (see Fig. 3c).

Bond valence sums calculated according to the method described in reference [12–13] confirm the trivalent states of all La atoms, and In(1) as well as In(2) in $La_5In_3S_9O_3$ (see Table 4). However, the bond valence calculated for In(3) is much higher than 3. As the In(3) site is occupied only at 15%, the In(3)–S distances are shorter than expected, which explains this discrepancy. For the S-deficient derivative $La_{10}In_6S_{17}O_{16}$ [5], we have calculated similar bond valence sums for La (3.02–3.23) and In (2.90–3.12) except for one indium atom, for which the valence sum is 1.70. This is in accordance with the formation of $(In_2)^{4+}$ pairs in this compound.
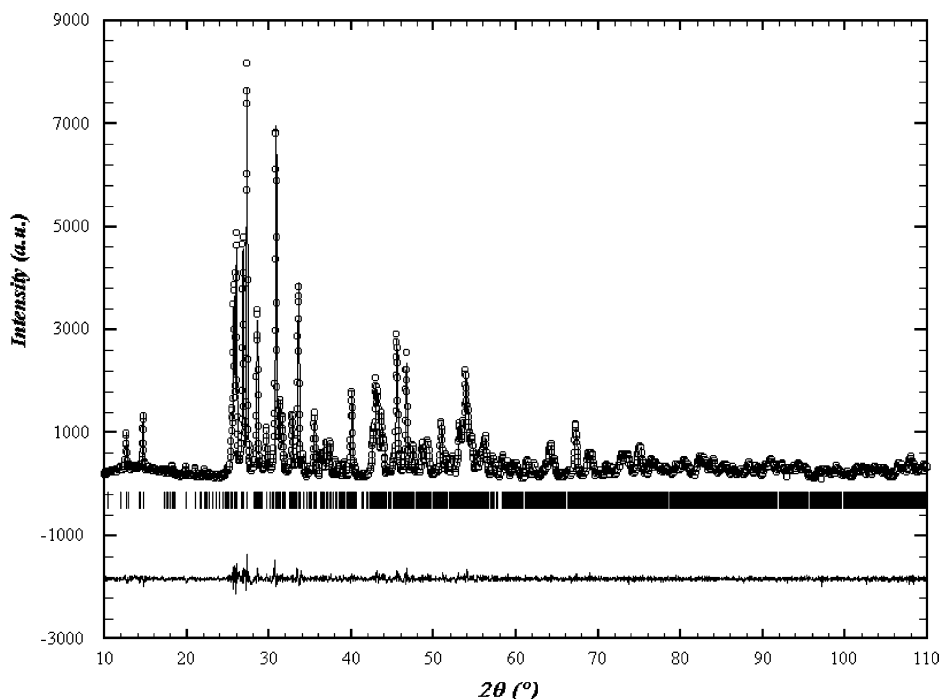
Fig. 1. Observed X-ray diffraction pattern recorded for LaInS$_2$O (open circle). In this picture the black line represents the calculated intensities obtained by profile matching, and the bottom curve shows the difference between experimental and calculated intensities.

Table 5
Positions ($2\theta°$) and relative intensities of the main diffraction peaks measured for LaInS$_2$O

$h\,k\,l$	2θ	I_{exp}	$h\,k\,l$	2θ	I_{exp}
2 2 0	14.70	12.8	5 2 1	33.55	53.2
2 4 0	25.49	13.6	7 2 1	40.01	13.9
1 2 1	25.72	43.8	0 6 1	42.99	24.1
6 0 0	26.00	56.9	1 6 1	43.22	20.7
2 2 1	26.82	57.2	8 2 1	43.63	10.2
3 4 0	27.30	100.0	0 0 2	45.50	32.8
3 2 1	28.55	40.1	4 6 1	46.64	17.1
4 4 0	29.66	10.3	9 4 0	46.67	12.7
4 2 1	30.83	94.3	6 0 2	53.16	14.5
2 5 0	31.32	15.2	3 4 2	53.88	24.3
3 3 1	31.62	13.7	5 8 0	54.17	14.2
7 2 0	32.78	14.4			

Fig. 2. Projection of the structure of La$_5$In$_3$S$_9$O$_3$ onto the (b, c) plane.

Fig. 4 shows the absorbance spectra of In$_2$S$_3$, LaInS$_2$O and La$_5$In$_3$S$_9$O$_3$ obtained after a Kubelka–Munk transformation [14]. The crossing point between the base line along the energy axis and the extrapolated line of the absorption edge gives the optical gap. For In$_2$S$_3$ and LaInS$_2$O, the optical gaps are respectively 2.24 and 2.73 eV. For the compound La$_5$In$_3$S$_9$O$_3$, the values are 2.60 eV (perpendicular to a) and 2.65 eV (parallel to a). These gap values explain the yellow color of both compounds. As shown in Fig. 5, optical gaps increase with the ratio O/(O+S) for In or La or mixed La/In compounds. According to the crystal structure study of La$_5$In$_3$S$_9$O$_3$, indium atoms are only bounded
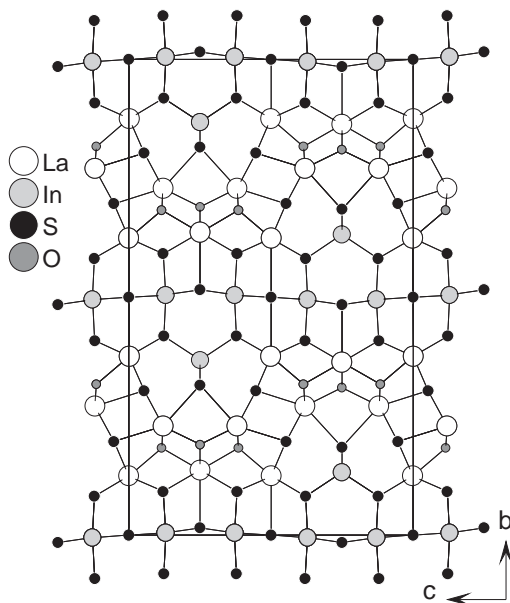
with S atoms in this compound while La is bonded to O and S atoms. We could expect the La oxychalcogenide part to give rise to an optical transition intermediate between those of La$_2$S$_3$ and La$_2$O$_2$S. This transition should be higher than the observed transitions for La$_5$In$_3$S$_9$O$_3$ and LaInS$_2$O. Consequently, the observed

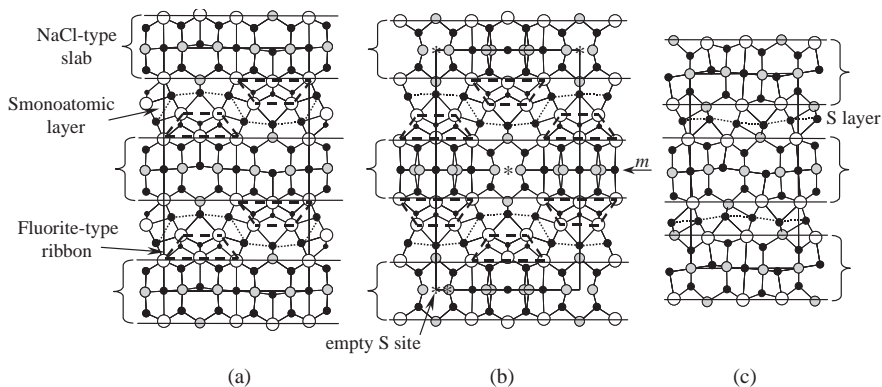Fig. 3. Modular description of the crystal structures of (a) $La_5In_3S_9O_3$, (b) $La_{10}In_6S_{17}O_6$ and (c) $La_4In_5S_{13}$. The fluorite-type ribbons and the three-atom-thick $(100)_{NaCl}$ layers are indicated on this figure as well as the S-monoatomic layer. Small black circle = O; large black circle = S; grey circle = In; empty circle = La.
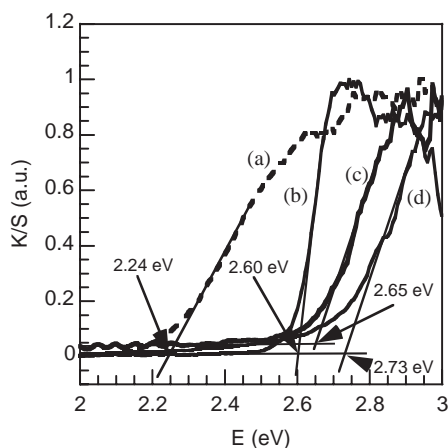

Fig. 4. Diffuse reflectance spectra of In_2S_3 (a) and $LaInS_2O$ (d) obtained after a Kubelka-Munk transformation at room temperature (K/S vs. E). Polarized transmitted light spectra of $La_5In_3S_9O_3$ measured with the polarization directions perpendicular (b) and parallel (c) to the a-axis.

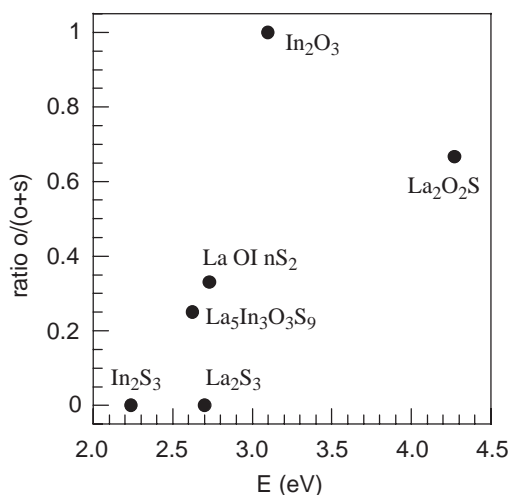Fig. 5. Optical gaps of $La_5In_3S_9O_3$ and $La_{10}In_6S_{17}O_6$ compared to those of In_2S_3, In_2O_3, La_2S_3 and La_2O_2S. The gaps are plotted versus the ratio of oxygen over all anions $O/(O+S)$.

transitions may be related to the In/S part and the optical gap increase observed from In_2S_3 to $La_5In_3S_9O_3$ or $LaInS_2O$ could result from the inductive effect of the associated, more electropositive, La cation.

3. Conclusions

During our investigation of the La–In–S–O quaternary system we could not find a transparent composite-like oxysulfide. However, we have found two new yellow compounds, namely $LaInS_2O$ and $La_5In_3S_9O_3$. The structure of $La_5In_3S_9O_3$ exhibits $La_{1.5}In_{1.5}S_3$ infinite [NaCl] type layers and $[La_5O_3]$ fluorite-type ribbons. Both building blocks are also present in the structure of the lanthanum and indium oxysulfide $La_{10}In_6S_{17}O_6$. It is most likely that the structure determination of $LaInS_2O$ would also reveal such blocks. We have measured the optical gaps for $LaInS_2O$ and $La_5In_3S_9O_3$ and we have found 2.73 and 2.60 eV, respectively. These gaps are intermediate between those of In_2S_3 and In_2O_3. As the indium atoms are connected preferentially to sulfur atoms, it seems difficult to get a transparent compound in the La–In–S–O system.

References

[1] D.S. Ginley, C. Bright, Transparent conducting oxides, MRS Bull. 25 (8) (2000) 15–65.
[2] K. Ueda, S. Inoue, S. Hirose, H. Kawazoe, H. Hosono, Appl. Phys. Lett. 78 (2001) 2333.
[3] M. Palazzi, C.R. Acad. Sci. Paris 292 (1981) 789–791.
[4] S. Inoue, K. Ueda, H. Hosono, N. Hamada, Phys. Rev. B 64 (2001) 1–5.
[5] L. Gastaldi, D. Carré, M.P. Pardo, Acta Crystallogr. B 38 (1982) 2365–2367.
[6] Brucker, SHELXTL, Brucker AXS Inc., Madison, WI, USA, 1998.
[7] S. Jaulmes, Acta Crystallogr. B 34 (1978) 2610–2612.

[8] S. Jaulmes, A. Mazurier, M. Guittard, Acta Crystallogr. C 39 (1983) 1594–1597.

[9] M. Guittard, S. Benazeth, J. Dugué, S. Jaulmes, M. Palazzi, P. Laruelle, J. Flahaut, J. Solid State Chem. 51 (1984) 227–238.

[10] J. Rodriguez-Carvajal, Program FullProf, Version 3.5d, 1998.

[11] G.G. Guseinov, F.H. Mamedov, H.S. Mamedov, Dokl. Akad. Nauk Az. SSR 35 (1979) 50–53.

[12] N.E. Brese, M. O'Keefe, Acta Crystallogr. Sect. B 47 (1991) 192–197.

[13] I.D. Brown, in: M. O'Keeffe, A. Navrostsky (Ed.), The Bond Valence Method, Structure and Bondings in Crystals II, Academic Press, New York, 1981.

[14] W.W. Wendlandt, H.G. Hecht, Reflectance Spectroscopy, Intersciences New York, 1966.